Petroleum 5 (2019) 206–213

Contents lists available at ScienceDirect

Petroleum

journal homepage: www.keaipublishing.com/en/journals/petlm

Pipeline wax deposition modeling: A sensitivity study on two commercial software

Giancarlo Giacchetta [a], Barbara Marchetti [b], Mariella Leporini [a, *], Alessandro Terenzi [c], Davide Dall'Acqua [a], Laura Capece [a], Roberta Cocci Grifoni [d]

[a] Dipartimento di Ingegneria Industriale e Scienze Matematiche (DIISM), Università Politecnica della Marche, via Brecce Bianche, Ancona, Italy
[b] Facoltà di Ingegneria, Università degli Studi E-Campus, via Isimbardi 10, 22060 Novedrate, CO. Italy
[c] Saipem S.p.A., via Toniolo 1, 61032, Fano, PU, Italy
[d] School of Architecture and Design, Università di Camerino, Camerino, MC, Italy

ARTICLE INFO

Article history:
Received 8 August 2017
Received in revised form
6 October 2017
Accepted 12 December 2017

ABSTRACT

This paper presents the results of a sensitivity study carried out to investigate the performances of two commercial codes, OLGA and LedaFlow, used to model the wax deposition process in pipelines under multiphase flow. Reliable simulations of the phenomenon are essential to properly design pipelines and to adopt cost-effective strategies for prevention and removal of wax deposits, reducing the risks of blockage. The main limit of the available models is that their predictions depend on a number of parameters which are usually adjusted to fit the experimental data obtained from laboratory deposition tests. Since a reliable upscale criterion has not been developed yet, model predictions have been more suitably validated using real field data, reported in literature. The performances of the commercial codes in modelling wax precipitation and deposition have been compared to each other.

1. Introduction

Wax deposition is a significant operational and economic concern in the Oil & Gas industry, leading to decreased production rates, equipment breakdowns and production shutdowns. Petroleum reservoir fluids are multicomponent mixtures consisting primarily of hydrocarbons, which can be divided into different groups such as paraffins, naphthenes and aromatics [1]. High molecular weight paraffins, with carbon numbers usually greater than 20, represent the waxy components of the crude oil. These components, at reservoir conditions, are dissolved in the petroleum fluid; however, as the crude oil flows towards the processing facilities and gradually becomes colder, the solubility of the paraffin molecules drops. If the temperature of the fluid falls below the Wax Appearance Temperature (WAT), the waxy components precipitate out of the liquid phase, crystalize and deposit on the pipe walls, thereby restricting the flow [2]. Thermal conditions, along with the crude oil chemical composition, represent the most influential parameter that determines whether wax deposition will occur. For that reason, issues related to wax deposition have become even more challenging in the late twentieth century, when the production of petroleum fluids shifted from onshore towards offshore reservoirs, where relatively low temperatures can lead to wax precipitation [3].

In literature, several deposit formation mechanisms have been proposed, namely molecular diffusion, shear dispersion, Brownian diffusion and gravity settling [4–6]; molecular diffusion is universally acknowledged as the dominant one, whereas the other mentioned mechanisms have been identified to have an insignificant impact on the phenomenon.

The wax deposition process, driven by molecular diffusion, can be summarized in the following five steps:

* Corresponding author.
E-mail addresses: g.giacchetta@univpm.it (G. Giacchetta), barbara.marchetti@uniecampus.it (B. Marchetti), m.leporini@univpm.it (M. Leporini), alessandro.terenzi@saipem.com (A. Terenzi), d.dallacqua@pm.univpm.it (D. Dall'Acqua), l.capece@pm.univpm.it (L. Capece), roberta.coccigrifoni@unicam.it (R. Cocci Grifoni).

Peer review under responsibility of Southwest Petroleum University.

Production and Hosting by Elsevier on behalf of KeAi

https://doi.org/10.1016/j.petlm.2017.12.007

(1) precipitation of dissolved wax molecules and formation of an incipient deposit layer on the pipe wall surface;
(2) generation of a radial concentration gradient of dissolved waxy components, which results in the diffusion of paraffin molecules from the bulk oil toward the wall;
(3) precipitation of waxy components on the surface of the existing deposit, which contributes to the growth of its thickness;
(4) internal diffusion of paraffin molecules inside the deposit layer, which leads to an increase in the solid wax fraction of the deposit;
(5) counter-diffusion of dewaxed oil out of the deposit.

The fourth and fifth steps lead to the increase in the solid wax fraction of the deposit, a phenomenon known as “deposit aging”.

To deal with wax problems, various methods for prevention and/or removal of paraffin deposits may be employed, such as insulation, active heating, wax-repellent surfaces, pigging, chemical treatments, cold flow technologies, fused-chemical reactions and biological treatments.

Conventionally, the measurement of the pressure drop occurring between two pipe sections is used to roughly estimate the thickness of the wax deposit and, consequently, decide on management strategies. Nevertheless, an accurate modelling of the phenomenon would be extremely useful to properly design pipelines and to perform economically viable remedial actions, based on reliable predictions. In order to correctly predict and describe the wax deposition phenomenon, various commercial tools have been developed. However, very few data relating to validations of these codes with field data are present in literature and often they have been compared with laboratory data, not representing the real field conditions. In a previous work [7], Bagatin et al. used several commercial codes to simulate the wax deposition phenomenon under single-phase flow. They compared the results to each other and with field data and they concluded that the software considered were not enough accurate to predict deposits in terms of thickness, pipeline location and composition as a function of time.

The purpose of this study is to investigate the current performances of two commercial codes, OLGA v2016.1 (OLGA Dynamic Multiphase Flow Simulator, Schlumberger, Houston, TX, USA) and LedaFlow v2.1 (Kongsberg Gruppen ASA Kirkegårdsveien 45 NO-3616 Kongsberg Norway), in modelling the wax deposition process in pipelines, under multiphase flow, and in reproducing a real field case reported in literature [8].

2. Material and methods

2.1. OLGA's wax deposition models

OLGA by Schlumberger is the industry standard tool for transient simulation of multiphase petroleum production [9]. It includes a wax deposition module, which allows to reproduce the wax deposition phenomenon, using one of the three models implemented, namely RRR, Matzain and Heat Analogy.

2.1.1. RRR model

The RRR (Rygg, Rydahl and Rønningsen) model is a multiphase flow wax deposition model which predicts wax deposition in wells and pipelines. It is a semi-stationary model since wax deposition build-up is a slower process than flow disturbances in a pipeline and it is not applicable for laminar flow [10]. Molecular diffusion and shear dispersion effect are considered the only mechanisms responsible for wax deposition. The volume rate of wax deposition by molecular diffusion for a wax-forming component i is calculated by Eq.(1):

$$Vol_{wax}^{diff} = \sum_{i=1}^{N_{wax}} \frac{D_{wo,i}(C_{wb,i} - C_{ws,i}) S_{wet} M_{wax,i}}{\delta_{lam} \rho_{wax,i}} 2\pi r_s L \tag{1}$$

Where:

N_{wax} is the number of wax components.

$D_{wo,i}$ is the diffusion coefficient calculated with Hayduk-Minhas correlation (m^2/s) [11].

$C_{wb,i}$ and $C_{ws,i}$ are the molar concentrations of the wax component i dissolved in the oil phase in the bulk and at the deposit surface respectively (mol/m^3).

S_{wet} is is the wetted fraction of the circumference.

$M_{wax,i}$ is the molar weight of wax component i (kg/mol).

δ_{lam} is the thickness of the laminar sub-layer (m).

$\rho_{wax,i}$ is the density of wax component i (kg/m^{30}).

r_s is the current inner pipe radius (m).

L is the length of the pipe section (m0).

The volume rate of wax deposited by shear dispersion is estimated from the following correlation of Burger et al. [6] (Eq.(2)):

$$Vol_{wax}^{shear} = \frac{k^* C_{ws} \dot{\gamma} A}{\rho_{wax}} \tag{2}$$

Where:

k^* is the shear deposition rate constant (kg/m^2).

C_{ws} is the volume fraction of precipitated wax in the oil at the inner wall temperature.

$\dot{\gamma}$ is the shear rate at the wall (s^{-1}).

A is the surface area available for deposition (m^2).

ρ_{wax} is the average wax density (kg/m^3).

When accounting for both mechanisms, the total rate of increase in thickness for the wax layer, $\dot{\delta}$, is given by Eq.(3):

$$\dot{\delta} = \frac{Vol_{wax}^{diff} + Vol_{wax}^{shear}}{(1 - \phi_{wax}) 2\pi r_s L} \tag{3}$$

ϕ_{wax} represents the porosity of the wax deposit, which is an adjustable parameter and is usually assumed to be in the range 0.6–0.9 [12].

The thickness of the wax layer is averaged around the pipe circumference, even if the inner pipe surface is only partially wetted with liquid.

The RRR model does not take into account the removal of wax from wall, in high velocity flows, due to the shear stress exerted by the oil; nevertheless, it implements a dissolution model of the wax deposited on the pipe wall. The model calculates the dissolved wax concentration derivative with respect to temperature, dC_w/dT, at the corresponding WAT for the pressure in the section. The dissolved wax concentration at the deposit surface is adjusted when the deposit surface temperature is above the Wax Dissolution Temperature (WDT), given in Eq.(4):

$$\mathrm{WDT} = WAT + \Delta T_{dissolution} \tag{4}$$

The dissolution temperature difference, $\Delta T_{dissolution}$, may be a constant or a function of the section pressure. The adjustment of the dissolved wax concentration at the deposit surface is obtained with Eq. (5):

$$C_{ws} = C_{w,T_s} + \left.\frac{dC_w}{dT}\right|_{WAT} (T_s - WDT) \tag{5}$$

Where $C_{w,Ts}$ is the wax concentration at the deposit surface temperature T_s. The adjusted C_{ws} is then used in the normal diffusion equation, in which (C_{wb}–C_{ws}) is the driving potential of the

diffusion process: only when C_{ws} is higher than C_{wb} the melting occurs. However, the total dissolution and diffusion rate of wax from wall to bulk is limited upwards [9].

2.1.2. Matzain model

The Matzain is a semi-empirical model, which incorporates a wax reducing mechanism, known as shear stripping, alongside molecular diffusion and shear dispersion to simulate wax deposition [4] [10]. In this model, shear dispersion is considered of minor importance in respect to RRR model.

The rate of wax build up is calculated by an empirical modification of Fick's law (Eq. (6)):

$$\frac{d\delta}{dt} = \frac{\Pi_1}{1+\Pi_2} D_{wo}\left[\frac{dC_w}{dT}\frac{dT}{dr}\right] \tag{6}$$

Where:

δ is the thickness of wax layer deposited on the wall (m).

D_{wo} is the diffusion coefficient calculated with the Wilke and Chang correlation [13](-)

C_w the concentration of wax in solution (weight %)

r is the pipe radial distance (m).

T is the fluid temperature (°C).

Eq.(7) is the supplied empirical correlation for $\Pi 1$, accounting for the porosity effect on the rate of wax build up and for other deposition enhancement mechanisms not considered by the diffusion coefficient.

$$\Pi_1 = \frac{C_1}{1 - C_L/100} \tag{7}$$

The constant C_1 is equal to 15 whereas C_L defines the amount of oil trapped in the wax layer, as shown in Eq.(8):

$$C_L = 100\left(1 - \frac{N_{\mathrm{Re}}^{0.15}}{8}\right) \tag{8}$$

The dimensionless parameter N_{Re} is a function of the effective inside radius of the pipeline:

$$N_{Re} = \frac{\rho_{oil} v_{oil} 2r_s}{\mu_{oil}}$$

Π_2 accounts for the wax limiting effect of shear stripping and is defined in Eq.(9):

$$\Pi_2 = 1 + C_2 N_{SR}^{C_3} \tag{9}$$

where $C_2 = 0.055$ and $C_3 = 1.4$.

The flow regime dependent Reynolds number (N_{SR}) is calculated for each regime as shown below.

$$N_{SR} = \frac{\rho_{oil} v_{oil} \delta}{\mu_{oil}} \text{ Single phase and stratified wavy flow}$$

$$N_{SR} = \frac{\rho_{mix} v_{oil} \delta}{\mu_{oil}} \text{ Bubble and slug flow}$$

$$N_{SR} = \frac{\sqrt{\rho_{mix}\rho_{oil}} v_{oil} \delta}{\mu_{oil}} \text{ Annular flow}$$

These expressions show that the shear stripping effect has been modelled as dependent on the wax layer thickness, flow conditions and flowing fluid properties. The thermal gradient of the laminar sub layer for deposition is given by Eq.(10):

$$\frac{dT}{dr} = \frac{(T_b - T_{ws})}{k_{oil}} h_h \tag{10}$$

Where k_{oil} is the thermal conductivity of the oil, h_h the inner wall heat transfer coefficient, T_b is the bulk fluid temperature and T_{ws} the deposit surface temperature.

2.1.3. Heat analogy

The third wax deposition model implemented in OLGA, i.e. the heat analogy, is not described in detail in the software user manual [9]. From a critical literature review, it has emerged that it calculates the mass transfer rate of wax employing the heat transfer analogy [12]. The heat transfer rate is given by:

$$\dot{Q} = h(T_{wb} - T_{ws}) \tag{11}$$

where h is the heat transfer coefficient. Similarly, the mass transfer rate of the component i can be expressed as:

$$\dot{M}_i = m_i(C_{wb,i} - C_{ws,i}) \tag{12}$$

where m_i is the mass transfer coefficient. The heat transfer coefficient is obtained from the Nusselt number (N_{Nu}), that is estimated from the Reynolds (N_{Re}) and Prandtl numbers (N_{Pr}):

$$\mathrm{h} = \frac{\lambda N_{Nu}}{2R} \tag{13}$$

$$N_{Nu} = f(N_{Re}, N_{Pr}) \tag{14}$$

Where $N_{Re} = \rho v d/\mu$ and $N_{Pr} = C_p\mu/\lambda$. The mass transfer coefficient, instead, is calculated from the Sherwood number ($N_{Sh,i}$), which is assumed to be a function of the Reynolds and the Schmidt numbers ($N_{Sc,i}$):

$$m_i = \frac{D_{wo,i} N_{Sh,i}}{d} \tag{15}$$

$$N_{Sh,i} = f(N_{Re}, N_{Sc,i}) \tag{16}$$

Where $N_{Sc,i} = \mu/\rho D_{wo,i}$.The analogy states that the functions in Eqs. (*14*) and (*16*) are identical. There are several different forms proposed in literature; an example is the Chilton-Colburn analogy, shown in Eqs. (*17*) and (*18*), used for many chemical engineering problems [14]:

$$N_{Nu} = 0.023\, N_{\mathrm{Re}}^{0.8} N_{\mathrm{Pr}}^{1/3} \tag{17}$$

$$N_{Sh,i} = 0.023\, N_{\mathrm{Re}}^{0.8} N_{\mathrm{Sc,i}}^{1/3} \tag{18}$$

In OLGA user manual [9], it is reported that the diffusion coefficient $D_{wo,i}$ is calculated using the Hayduk&Minhas correlation [11]; moreover it is stated that the Heat Analogy model, like the RRR, includes the shear deposition effect, and, like the Matzain, it takes into account the shear stripping phenomenon.

2.2. LedaFlow's wax deposition model

LedaFlow by Kongsberg is a transient multiphase flow simulator; like OLGA, it includes a module which allows to simulate wax deposition phenomenon. This software implements a simplified 1D wax deposition model, based on Lee's thesis [14], that is not described in detail in the software user manual [15]. Two processes are modelled:

- wax crystallization, forming a wax slurry in which wax particles are suspended in oil phase;
- wax deposition on pipe wall, responsible for the creation of wall deposit.

The radial diffusion of the dissolved wax molecules causes the build-up of the wax deposit: the concentration difference (C_{wb} - C_{ws}) represents the mass transfer driving force.

In most of the industrial wax models, the wax concentrations in the bulk and at the deposit surface are determined using the wax solubility curve, obtained inverting the wax precipitation curve. The transformation is based on the fact that the amount of wax that remains soluble in the liquid phase should be equal to the total wax content minus the amount of wax that has precipitated [3]. However, in this way, the wax solubility concentrations are given by their thermodynamic equilibrium values, which is not generally valid [16]. Lee [14] introduces a kinetic precipitation term (Eq.(19)) to account for the kinetics of the precipitation of the dissolved wax molecules on the boundary layer of the fluid:

$$r = k_r\left[C - C^{sat}(T)\right] \tag{19}$$

where k_r is the precipitation rate constant. Since the precipitated wax crystals are found to most likely flow with the oil instead of depositing on the pipe wall, they are assumed not to contribute to the formation of wax deposit. Consequently, a higher precipitation rate leads to less deposition on the pipe wall because it reduces the amount of dissolved waxy component potentially available for diffusion towards the pipe wall. The precipitation rate constant is obtained using Eq.(20):

$$k_r = k_d A_p \rho_n = \left(\frac{Sh_p \cdot D_{wo}}{d_p}\right) A_p \rho_n \tag{20}$$

Where k_d is the mass transfer coefficient from bulk to the individual nucleus surface, A_p is the surface area of a nucleus and ρ_n is the number density of wax nuclei. k_d can be calculated from Eqs. (*21*) and (*22*):

$$k_d = \frac{Sh_p \cdot D_{wo}}{d_p} \tag{21}$$

$$Sh_p = 2 + 0.6\, Re_p^{0.5} Sc_p^{(1/3)} \approx 2 \tag{22}$$

where Sh_p, Re_p and Sc_p are, respectively, the Sherwood, Reynolds and Schmidt numbers of the particle and d_p is its critical nucleus size. The diffusion coefficient, D_{wo}, is calculated using the Hayduk and Minhas correlation [11]. The model implemented in LedaFlow also supports the melting of wax, which increases the amount of wax dissolved in oil.

2.3. Field data

To evaluate the performances of the two software, it has been decided to compare simulation results with the data of a Petrobras field in Campo Basin, presented by Noville and Naveira [8]. The wells of Petrobras field in Campo Basin produce in a water depth higher than 800 m. Three wells (A, B and C) which flow with topside arrival temperature below the WAT, have been analysed by Noville and Naveira, however only one well (well B) is equipped with two pressure and temperature sensors (TPT and PDG) and in fact Noville and Naveira reported only field data relating to this well on their work. For this reason, in the present study only the well B case has been simulated, trying to reproduce the pressure behaviour at PDG (Permanent Downhole Gauge, installed in the tubing, close to the reservoir), shown in Fig. 1. A subsea pipeline transports a multiphase (gas-oil-water) flow from the well B to a central processing facility. The pipeline is 7.5-km long and has a variable internal diameter (125 mm and 150 mm). Table 1 summarises the main characteristics of well B.

Wax appearance temperature of the crude is about 17 °C and the Wax Precipitation Curve and the molar composition of the wax fractions are reported in the study of Noville and Naveira [8].

2.4. Sensitivity analyses

The study of the wax deposition models implemented in the software reveals that their predictions strongly depend on several empirical parameters; for that reason, a sensitivity analysis has been carried out in order to evaluate the effect of each parameter on wax deposition. Table 2 and Table 3 show the values adopted for each adjustable variable, respectively in OLGA and in LedaFlow. Note that the wax deposition models do not employ the same parameters, so two different batch of simulations have been run with the two software. It has been decided to reproduce with OLGA v2016.1 the same sensitivity analysis carried out by Noville and Naveira [8] with OLGA v5.3 in order to try to reproduce their field data. It is important to specify that Noville and Naveira concluded that the simulations carried out could not represent the global field pressure behaviour but only the period where the diffusion mechanism is dominant.

3. Results and discussion

Fig. 2 shows the impact of the diffusion coefficient multiplier on wax deposit thickness: as expected, higher values of that parameter produce thicker deposits and, consequently, greater increments of pressure at inlet (Fig. 3). However, the results obtained are quite different from those published by Petrobras: using OLGA 2016 the wax deposit, after a simulation time of 50 days, is not as thick and extended as the one simulated with OLGA 5.3. After a critical review of all the OLGA new versions' release notes distributed by Schlumberger, it has been concluded that two important modifications have been implemented into the wax deposition module, in particular:

- the calculation of wax/oil dispersion viscosity has been changed to the calculation described in [17] by Pedersen and Rønningsen;
- in previous versions of OLGA, the output variable DXWX (i.e. thickness of wax layer deposited at wall) was based on the wrong density and, thus, overestimated.

Regarding the other parameters analysed, the same conclusions as Noville and Naveira's [8] may be drawn:

(1) the wax roughness has a negligible impact on the thickness of the deposit, but higher values of this parameter produce larger increments of the pressure at inlet;
(2) the wax deposit thickness estimated using the RRR model is nearly 10 times lower than that obtained using the Matzain model: after a simulation time of 50 days, the former has reached a value of 0.57 mm, whereas the latter a value of 5.32 mm. Therefore, in the RRR case, the deposit is too thin to produce an increment of the pressure at inlet, which, in fact, remains almost constant, while, in the Matzain case, the pressure rises by roughly 1 bar. Since field data show a significant increase in pressure due to wax deposition, the

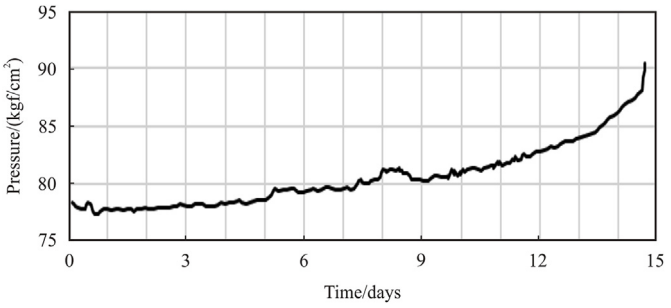

Fig. 1. Pressure behaviour at PDG of well B [8].

Matzain model seems to reproduce the phenomenon better than the RRR;

(3) the wax porosity greatly affects wax deposit thickness; in fact, this parameter represents the fractional amount of trapped oil in the deposit, thus, the higher it is, the thicker the deposit becomes;

(4) the values of shear multipliers have a great impact on the thickness and the extension of wax deposit; in particular, it has been observed that, setting at 0 the shear multiplier of C2, wax deposition is highly enhanced, since the shear stripping effect, in this way, is not taken into account. On the contrary, higher values of these two multipliers increase the wax deposition limiting effect of shear and result in thinner deposits. As a consequence, these parameters affect also the

Table 1
Main characteristics of well B.

API^0	GOR$_f$ (sm^3/sm^3)	Flow rate (m^3/d)		Pressure (kgf/cm^2)			Temperature (°C)		
		Liquid	Gas lift	Platform	Reservoir	Saturation	Platform	Reservoir	WAT
26.6	110	416	163191	11.9	156.9	139	5	78	17.1

Table 2
Values of wax deposition parameters used in OLGA.

Parameter	Diffusion coefficient multiplier	Wax roughness	Deposition model	Wax porosity	Shear multiplier		Wax conductivity
					C2	C3	
Diffusion coefficient multiplier	1 5 10 50 100 1000	1	MATZAIN	0.9	1	1	0.242
Wax roughness	5	0 1	MATZAIN	0.9	1	1	0.242
Deposition model	5	1	RRR MATZAIN	0.9	1	11	0.242
Wax porosity	1	1	MATZAIN	0.9 0.2	1	1	0.242
Shear multiplier	100	1	MATZAIN	0.6	0 1 10	1 1 10	0.242
Wax conductivity	15	0	MATZAIN	0.6	0	1	0.242 0.016

Table 3
Values of wax deposition parameters used in LedaFlow.

Parameter	d23 [mm]	acwall	tfwall	tfwax	Viscosity parameters		
					A	B	C
Mean diameter of wax particles (d23)	0.005 0.01 0.02 0.04	1	1	1	1	20	0
Time acceleration factor for wall deposition (acwall)	0.01	1 2	1	1	1	20	0
Tuning factor for wall deposition (tfwall)	0.01	1	1 5 10	1	1	20	0
Tuning factor for crystallization in oil phase (tfwax)	0.01	1	1	1 5 10 50 1000	1	20	0
Viscosity parameters	0.01	1	1	1	1 0.00273	20 16.6	0 10.05

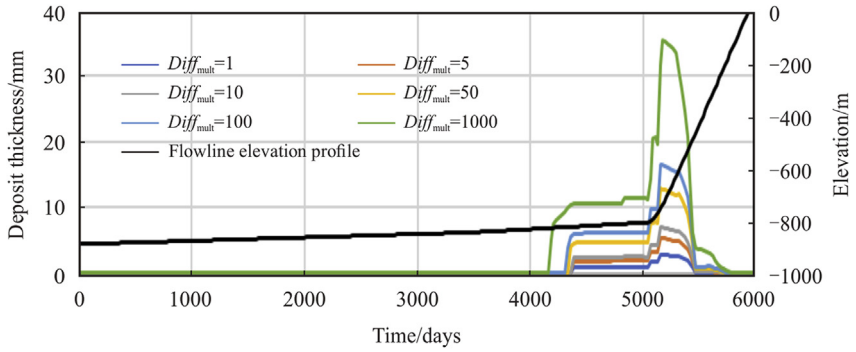

Fig. 2. Wax deposition profile varying the diffusion coefficient multiplier in OLGA.

pressure behaviour at inlet: without the shear stripping effect, the pressure at inlet rises from 75.5 bara to 110 bara, after a simulation time of 50 days, whereas, with default values, it reaches only 77.7 bara; intensifying the shear stripping effect, instead, the pressure remains almost constant;

(5) the wax conductivity, finally, seems to affect very little wax deposition phenomenon.

As far as Ledaflow is concerned, the sensitivity analysis has shown that:

(1) the parameter that most affects the wax deposit in terms of thickness is the tuning factor for wall deposition: it multiplies the deposition rate and, consequently, the higher it is, the thicker the deposit becomes. Fig. 4 shows the results obtained with different values of tfwall after a simulation time of 50 days;

(2) the tuning factor (tfwax) for crystallization in oil phase has a minor influence on the results of wax deposition simulations: higher values of tfwax increase the precipitation rate and, consequently, the amount of wax crystals that flow with the oil instead of depositing on the pipe wall, thus reducing the deposit thickness. Values of tfwax of 50 or 1000 produce two overlapping deposit profiles, suggesting that there is a threshold beyond which this parameter does not affect the simulation anymore;

(3) the time acceleration factor for wall deposition speeds up the wall deposition rate, without affecting the flow and the fraction of wax particles in the oil phase; it has been introduced in LedaFlow to reduce the required simulation time, since wax deposition is a very slow process. Fig. 5 displays the results obtained setting acwall at 2 and halving the simulation time;

(4) the viscosity parameters A, B and C affect the viscosity of the wax slurry, computed using the expression given by Eq.(23) [18]:

$$\frac{\mu}{\mu_0} = 1 + 2.5\phi + C\phi^2 + A(\exp(B\phi) - 1) \tag{23}$$

where ϕ is the volume fraction solids, μ_0 the viscosity of the suspending medium and any non-Newtonian effects are neglected.

The default values (A = 1, B = 20 and C = 0) have been used in the majority of the cases; one simulation, instead, has been run with the values reported in Thomas' article [18] (A = 0.00273, B = 16.6 and C = 10.05): from the comparison of the results, it has emerged that these parameters have a negligible effect on wax deposit profile;

(5) the mean diameter of wax particles is a variable that plays a role in the formation of the wax crystals in oil and it seems to greatly affect the shape and, to a lesser extent, the thickness of the wax deposit, as shown in Fig. 6.

Fig. 7 displays the results of the two base cases, that have been run in OLGA and in LedaFlow setting all the wax deposition parameters at their default values. In both cases, after a simulation time of 50 days, the deposit thickness is quite small: it reaches a value of 2.80 mm in OLGA and of 1.97 mm in LedaFlow. As a result, the pressure behaviour at inlet, simulated by OLGA, shows an increase of only 0.5 bar (from 75.7 to 76 bara). Instead, LedaFlow presents a constant pressure at PDG (75.17 bara) and, thus, it is not able to reproduce the pressure increment at inlet: this software, in

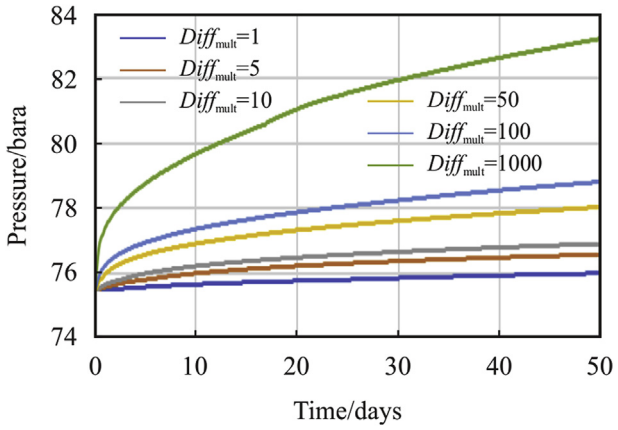

Fig. 3. Pressure at PDG varying the diffusion coefficient multiplier in OLGA.

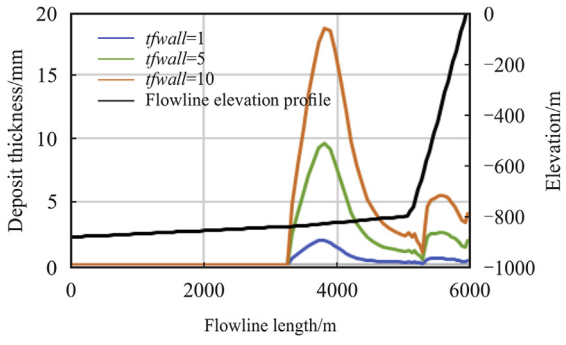

Fig. 4. Wax deposition profile varying tfwall in LedaFlow.

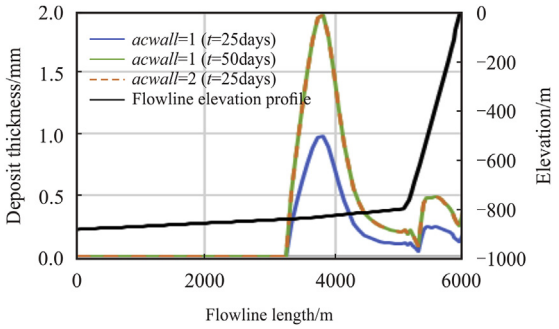

Fig. 5. Wax deposition profile varying acwall in LedaFlow.

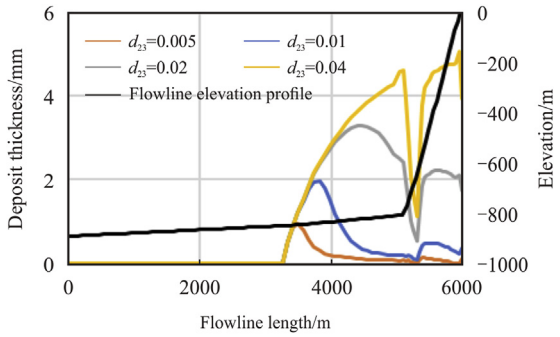

Fig. 6. Wax deposition profile varying d23 in LedaFlow.

fact, does not model the change in cross-sectional area with wax deposit formation. This simplified approach probably has to be ascribed to the fact that the declared main objective of LedaFlow is to determine the required pigging frequency to keep production going [15]: considering that, generally, commercial pipes are pigged whenever the deposit thickness reaches 2-5 mm, the flow restriction is not taken into account by this software. Therefore, it has not been possible to accomplish the initial purpose and validate LedaFlow predictions with available pressure field data. On the other hand, OLGA results, in terms of pressure at PDG, have been compared with sensors data: it has been observed that neither this software is able to properly reproduce field data, anyway, Fig. 8 shows that the pressure curve, obtained setting the diffusion coefficient multiplier at 100, can represent quite well the pressure behaviour in the first period (nearly five days). Instead, OLGA seems unable to reproduce the subsequent exponential trend of pressure that Noville and Naveira in [8] attribute to another hypothetical mechanism, prevailing over molecular diffusion.

Furthermore, by comparing the two wax deposit profiles in Fig. 7, it can be noticed that in LedaFlow simulation the wax deposition begins before along the flowline profile. This is due to the fact that the only thermodynamic input required for wax deposition model, in this software, is a user-given Wax Precipitation Curve (WPC), which can be obtained from a fluid program, such as PVTsim or Multiflash, and refers to a specific pressure. Ledaflow, therefore, does not consider the influence of pressure on WAT and on the amount of wax precipitated: paraffins begin to precipitate when the fluid temperature falls below the WAT, identified by the given WPC, independently from the pipeline pressure. OLGA, on the contrary, requires a pre-calculated wax table (generated, as well as the WPC, in a fluid program such as PVTsim or Multiflash) which contains data on each of the wax forming components, at different values of temperature and pressure. Then, in OLGA, pressure affects the WAT and wax begins to precipitate when the fluid temperature falls below the wax appearance temperature at the corresponding pressure in the section.

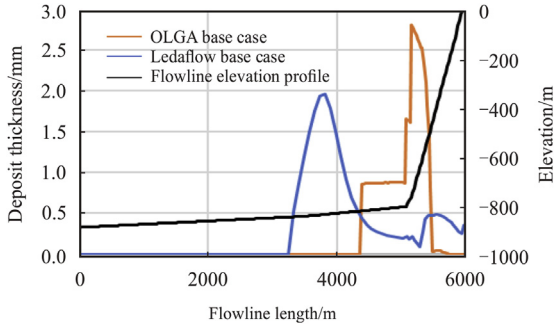

Fig. 7. Comparison of wax deposition profiles of OLGA and LedaFlow base cases.

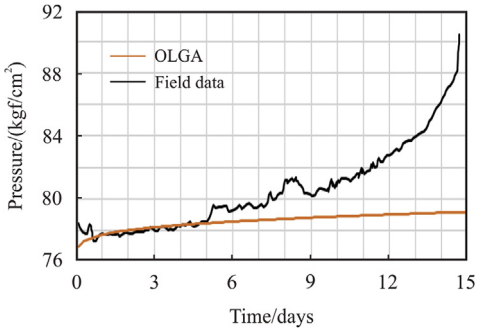

Fig. 8. Pressure comparison between field data and OLGA simulation.

4. Conclusions

In this paper, the performances of OLGA and LedaFlow in modelling wax deposition have been investigated. Two sensitivity analyses have been carried out in order to evaluate the effect of each adjustable variable on wax deposition. The two software, then, have been used to reproduce the data of a Petrobras field in Campo Basin. LedaFlow has shown two main limits: it does not consider the influence of pressure on WAT, which determines the beginning of wax precipitation, and it does not model the flow restriction due to wax deposit formation, thus proving to be unable to reproduce the pressure increment at inlet. Neither OLGA has been able to properly simulate the pressure behaviour at PDG; anyway, it has been observed that, by setting the diffusion coefficient multiplier at 100, this software can reproduce the pressure trend at inlet in the first period. The authors will further investigate which mechanism may be responsible of the exponential trend of pressure observed in the second period, and how it can be modelled in the software.

References

[1] K.S. Pedersen, P.L. Christensen, Phase Behavior of Petroleum Reservoir Fluids, CRC Press Taylor & Francis Group, 2007.
[2] R. Venkatesan, N. Nagarajan, K. Paso, Y. Yi, A. Sastry, H. Fogler, The strength of paraffin gels formed under static and flow conditions, Chem. Eng. Sci. 60 (2005) 3587–3598.
[3] Z. Huang, S. Zhen, H.S. Fogler, Wax Depostion - Experimental Characterizations, Theoretical Modeling, and Field Practices, CRC Press, 2015.
[4] A. Aiyejina, D.P. Chakrabarti, A. Pilgrim, M.K.S. Sastry, Wax formation in oil pipelines: a critical review, Int. J. Multiphas. Flow 37 (2011) 671–694.
[5] L.F.A. Azevedo, A.M. Teixeira, A critical review of the modeling of wax deposition mechanisms, Petrol. Sci. Technol. 21 (3) (2003) 393–408.
[6] E. Burger, T. Perkins, J. Striegler, Studies of wax deposition in the trans Alaska

pipeline, J. Petrol. Technol. 33 (6) (1981).
[7] R. Bagatin, C. Busto, S. Correra, M. Margarone, C. Carniani, Wax Modeling: There Is Need for Alternatives, SPE Russian Oil & Gas Technical Conference and Exhibition, Moscow, Russia, 2008.
[8] I. Noville, L. Naveira, Comparison between Real Field Data and the Results of Wax Deposition Simulation, SPE Latin American and Caribbean Petroleum Engineering Conference, Mexico City, Mexico, 2012.
[9] Schlumberger, OLGA, User Manual, 2016.
[10] K. Rosvold, Wax deposition models, Master thesis, NTNU - Norges teknisk-naturvitenskapelige universitet, 2008.
[11] W. Hayduk, B. Minhas, Correlations for prediction of molecular diffusivities in liquids, Can. J. Chem. Eng. 60 (1982) 295–299.
[12] B. Edmonds, T. Moorwood, R. Szczepanski, X. Zhang, Simulating wax deposition in pipelines for flow assurance, Energy Fuel. 22 (2008) 729–741.
[13] C. Wilke, P. Chang, Correlation of diffusion coefficients in dilute solutions, AIChE J. 1 (2) (1955) 264–270.
[14] H. Lee, Computational and Rheological Study of Wax Deposition and Gelation in Subsea Pipelines, PhD Thesis, University of Michigan, 2008.
[15] Kongsberg, LedaFlow 2.1.252.024 User Manual.
[16] O. Hernandez, H. Hensley, C. Sarica, M. Volk, Improvements in Single-phase Paraffin Deposition Modeling, SPE Annual Technical Conference and Exhibition, Denver, Colorado, USA, 2003.
[17] K.S. Pedersen, H.P. Rønningsen, Influence of wax inhibitors on wax appearance temperature, pour point, and viscosity of waxy crude oils, Energy Fuel. 17 (2003) 321–328.
[18] D. Thomas, Transport characteristics of suspension: a note on the viscosity of newtonian suspensions of uniform spherical particles, J. Colloid Sci. 20 (1965) 267–277.